Research Square

Preprints are preliminary reports that have not undergone peer review.
They should not be considered conclusive, used to inform clinical practice,
or referenced by the media as validated information.

Nearly continuous Ca^+ optical clocks with stability at the 10^-18 level

Yao Huang (yaohuang@wipm.ac.cn)
Innovation Academy for Precision Measurement Science and Technology, Chinese Academy of Sciences

Baolin Zhang
Innovation Academy for Precision Measurement Science and Technology, Chinese Academy of Sciences

Mengyan Zeng
Innovation Academy for Precision Measurement Science and Technology, Chinese Academy of Sciences

Huaqing Zhang
Innovation Academy for Precision Measurement Science and Technology, Chinese Academy of Sciences

Yanmei Hao
Innovation Academy for Precision Measurement Science and Technology, Chinese Academy of Sciences

Zheng Chen
Innovation Academy for Precision Measurement Science and Technology, Chinese Academy of Sciences

Miao Wang
Innovation Academy for Precision Measurement Science and Technology, Chinese Academy of Sciences

Hua Guan
Innovation Academy for Precision Measurement Science and Technology, Chinese Academy of Sciences

Kelin Gao
Wuhan Institute of Physics and Mathematics

Letter

Keywords: Frequency Stability, Operating Uptime Rate, Quasi-continuous Operation

Posted Date: March 11th, 2021

DOI: https://doi.org/10.21203/rs.3.rs-120082/v1

License: This work is licensed under a Creative Commons Attribution 4.0 International License.
Read Full License

Nearly continuous Ca^+ optical clocks with stability at the 10^{-18} level

Yao Huang[1,2], Baolin Zhang[1,2,3], Mengyan Zeng[1,2,3], Huaqing Zhang[1,2,3], Yanmei Hao[1,2,3], Chen Zheng[1,2,3], Miao Wang[1,2,3], Hua Guan[1,2], & Kelin Gao[1,2]

[1]*State Key Laboratory of Magnetic Resonance and Atomic and Molecular Physics, Innovation Academy for Precision Measurement Science and Technology, Chinese Academy of Sciences, Wuhan 430071, China*

[2]*Key Laboratory of Atomic Frequency Standards, Innovation Academy for Precision Measurement Science and Technology, Chinese Academy of Sciences, Wuhan 430071, China*

[3]*University of Chinese Academy of Sciences, Beijing 100049, China*

Optical clocks are important for precise measurements in the field of physics. As reported, both the instability and uncertainty of optical lattice clocks are more than two orders of magnitude smaller than those of the best microwave clocks. Therefore, in the near future, optical clocks could be used to redefine the second. Nevertheless, an optical clock with reliability comparable to microwave clocks has not been achieved thus far. In this paper, we compared the frequencies of two Ca^+ optical clocks that were nearly continuously operated for 31 days. Through the comparison experiment, the frequency stability of a single clocks was found to be 6.3×10^{-18} at an averaging time of 520 000 s and 7.9×10^{-18} at averaging time of 262000 s, while the operating uptime rate reached more than 90% in the period of around 5 days. Thus, our experiment demonstrated that it is possible to increase the stability of single-ion optical clocks to the 10^{-18} level, while still maintaining quasi-continuous operation with a high operating rate. This result further confirms that optical clocks can potentially be used to redefine the second.

In recent years, significant progress has been made in the development of optical lattice clocks and single-ion optical clocks. Uncertainties and instabilities in the orders of 10^{-18} and 10^{-19} have been achieved for these clocks [1-5], which are two orders of magnitude lower than those of a cesium fountain clock [6-8] that is used as the reference clock for the definition of the second. Therefore, scientists are considering the use of optical clocks to redefine the second [9]. However, high-precision optical clock systems are considerably more complicated in design than cesium fountain clocks, and often require simultaneous operation of several lasers. This complexity is the leading factor that prevents the use of optical clocks for defining the second instead of cesium fountain clocks. In particular, to ensure reproducibility of the definition of the second, several reference clocks are required internationally that can sustain long-term quasi-continuous operation [10-14]. Although different types of optical clocks with high accuracy in the order of 10^{-18} have been realized in many laboratories worldwide [1-5], to our knowledge, there are only a few reports on long-term quasi-continuous performance of the optical clocks [14, 15]. Considering this, extrapolation algorithms are required to account for the nonoperational time periods between working periods of the optical clocks in order to maintain a consistent international time scale [10-13]; alternatively, in these nonoperational time periods, the use of local oscillators (typically hydrogen masers) as flywheel clocks is necessary to maintain a consistent time scale. In the latter

case, the frequency fluctuations of the flywheel clocks become the primary source of uncertainty for frequency/time related measurements [10-12]. Speaking of optical clocks, an optical lattice clock with a stability as high as $2.2\times10^{-16}/\sqrt{\tau}$ has been recently reported [16]; this stability is significantly higher than that of the most stable single-ion optical clock ($\sim1.5\times10^{-15}/\sqrt{\tau}$ [1,17]). While in terms of uncertainty, compared with thousands of neutral atoms for reference in the optical lattice clocks, for single-ion optical clocks, with the single ion trapped in the electric field, the ion is in a more isolated environment and the frequency shifts can be more easily and precisely evaluated. The newly reported Al^+ optical clock has achieved an uncertainty in the order of 10^{-19} [1], which exceeds that of the best optical lattice clocks [5] thus far. To enable the use of these single-ion optical clocks with extremely low uncertainty for precise measurements or comparisons, currently, only two approaches exist, namely increasing their stability or averaging over longer effective times.

Furthermore, to avoid the measurement errors induced by the use of flywheel clocks, reliable optical clocks that can continuously operate for long periods must be constructed [14,15]. In particular, for single-ion clocks, their stability must be improved for long-term quasi-continuous operation to allow for measurements or comparisons with a precision in the order of 10^{-18}. In this paper, the frequency comparison between two Ca^+ optical clocks that were nearly continuously operated for more than a month is reported. The frequency stability of both optical clocks during operation spanning hundreds of thousands of seconds was found to be $< 7\times10^{-18}$ with uptime rates of more than 90% in the working period of around 5 days. This work demonstrates the possibility of achieving long-term, reliable, and nearly continuous operation of single-ion optical clocks.

Experimental Results

In 2015, the Wuhan Institute of Physics and Mathematics (WIPM) has built two Ca^+ optical clocks, hereinafter referred to as Clock 1 and Clock 2, respectively. In our previous report, by frequency comparing these two clocks, the overall uncertainty was found as 7×10^{-17} [18], which was lower than that of the best fountain clocks thus far, indicating that the system uncertainty of these two optical clocks is better than that of the fountain clocks. Moreover, the stabilities of the single clocks were measured as $1\times10^{-14}/\sqrt{\tau}$, reaching to the order of 10^{-17} after 20000 s of averaging. Recently, we further improved the performance of Clock 2 to an uncertainly of $1.3\sim2.2\times10^{-17}$ [19,20]; this uncertainty was primarily limited by the blackbody radiation shift due to the blackbody field temperature evaluation.

Compared with the uncertainties and stabilities of optical clocks referenced to Al^+, Yb^+, Sr, Yb, etc. [1-5], there is still considerable room for improvement in those of Ca^+ optical clocks. Nevertheless, it is important to note that Ca^+ optical clocks have some unique characteristics. Because all lasers used can be constructed using diode lasers, Ca^+ optical clocks are relatively simple to implement, low in cost, robust, and easy to realize for integrated and commercial applications. Therefore, the Ca^+ optical clock is an ideal candidate for construction of an optical clock time scale. For making the stability and the uptime rate better, targeting a clock with high uptime rate and 10^{-18} level stability, improvements on the optical clocks are made (see Methods). In order to further lower the instability and uncertainty of the Ca^+ optical clocks, we built another single-ion optical clock with a new design, referred to as Clock 3. Clock 2 is also improved. The stability and uncertainty are evaluated with frequency comparison of Clock 3 and Clock 2.

Up time rate of the clocks

The control programs for both Clocks 2 and 3 were designed to be automatic to enable long-term measurements. In particular, the control programs automatically implement peak locking after peak searching, error correction, relocking after optical-fiber noise elimination and unlocking, alarm after laser unlocking, and e-mail reminders, among others. Furthermore, the programs can automatically solve common unlocking problems encountered during the operation of the optical clocks. During automatic peak searching, first, a relatively strong detection optical power and short action time are applied to preliminarily determine the clock transition component frequencies using the Rabi method; then, the detection optical power is reduced and action time is increased for precise spectral line frequency determination for which the Ramsey method is used. The entire peak searching process takes about 10 s. Because the Ramsey method is prone to errors in detecting the fringe, the control program checks the frequency of the center of the Rabi spectral lines and that of the Ramsey spectral lines every 20 min. From January to March 2019, the two optical clocks were operated simultaneously for 31 days. During the experimental duration, aside from manual locking after laser unlocking, and about 10 min of monitoring every morning to check the micro-motion amplitude and ion temperature, no other human interference was made.

Fig. 1 shows the frequency difference measured of the two clocks. The single clock total Allan deviation for the 31-day-long clock run is shown in Fig 2. The overall uptime percentage is ~73%, during the last 5 days, the uptime is >90%. Especially in the night of March 10, the uptime is ~100% over ~6 hours.

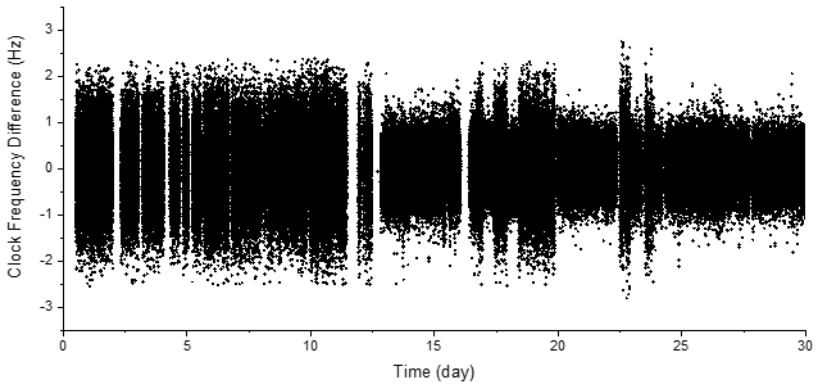

Fig. 1. the frequency difference measured of the two clocks. Each data point shows the frequency difference average in an 8-s-long experiment. During the 31-day-long clock comparison, transition pairs $^2S_{1/2}(m=\pm1/2)\rightarrow{}^2D_{5/2}(m=\pm1/2)$ and $^2S_{1/2}(m=\pm1/2)\rightarrow{}^2D_{5/2}(m=\pm3/2)$, or $^2S_{1/2}(m=\pm1/2)\rightarrow{}^2D_{5/2}(m=\pm1/2)$ and $^2S_{1/2}(m=\pm1/2)\rightarrow{}^2D_{5/2}(m=\pm5/2$ are chosen and switched for a few times during the clock running. The overall uptime percentage is ~73%, during the last 5 days, the uptime is >90%.

Stability measurement results

After the above-mentioned improvements, the two clocks are ready for comparison after the micromotion is minimized for both clocks. In the comparison, the two clocks share the same clock laser, which synchronize probe the two ions trapped in two ion traps. Each clock has its own lasers

except the clock laser; however, the laser system setups are identical. During the probing process, two 0.35-ms-long π/2 pulses are used, between which an 80-ms-long wait time is added with probe time switched off. All the other lasers are totally blocked by mechanical shutters during the probing process for eliminating the ac Stark shift. For each clock running cycle, the dead time (the overall time cost for laser cooling, state preparation, extra 3.7 ms for shutters, etc.) percentage is < 20%. The probing process is repeated for 15 times and the overall time costs for one comparison experiment is ~ 8 s.

For ions like Ca^+ or Sr^+, Zeeman components with different m_J sub levels have different sensitivity to the quadrupole shifts. By locking to multiple Zeeman components with different m_J sub levels, the quadrupole shift can be canceled out with a certain method [18, 21-23]. For Ca^+ clock, Zeeman transition pairs $^2S_{1/2}(m = \pm 1/2) \rightarrow {}^2D_{5/2}(m = \pm 1/2)$ and $^2S_{1/2}(m = \pm 1/2) \rightarrow {}^2D_{5/2}(m = \pm 3/2)$, or $^2S_{1/2}(m = \pm 1/2) \rightarrow {}^2D_{5/2}(m = \pm 1/2)$ and $^2S_{1/2}(m = \pm 1/2) \rightarrow {}^2D_{5/2}(m = \pm 5/2)$ are chosen to probe for cancelling both the quadrupole shift and the tensor Stark shift. While the quadrupole shift can be canceled out with these methods, different cancelation methods have different sensitivity to the quadrupole shifts variation. For instance, clocks locked to the $^2S_{1/2}(m = \pm 1/2) \rightarrow {}^2D_{5/2}(m = \pm 1/2)$ and $^2S_{1/2}(m = \pm 1/2) \rightarrow {}^2D_{5/2}(m = \pm 5/2)$ transition pairs are more immune to the quadrupole shift variation than locked to the $^2S_{1/2}(m = \pm 1/2) \rightarrow {}^2D_{5/2}(m = \pm 1/2)$ and $^2S_{1/2}(m = \pm 1/2) \rightarrow {}^2D_{5/2}(m = \pm 3/2)$ transition pairs. However, the $^2S_{1/2}(m = \pm 1/2) \rightarrow {}^2D_{5/2}(m = \pm 5/2)$ transition pair is also more linear Zeeman shift sensitive thus the clock running is more likely to be affected by the magnetic field variation. During the 31-day-long clock comparison, transition pairs $^2S_{1/2}(m = \pm 1/2) \rightarrow {}^2D_{5/2}(m = \pm 1/2)$ and $^2S_{1/2}(m = \pm 1/2) \rightarrow {}^2D_{5/2}(m = \pm 3/2)$, or $^2S_{1/2}(m = \pm 1/2) \rightarrow {}^2D_{5/2}(m = \pm 1/2)$ and $^2S_{1/2}(m = \pm 1/2) \rightarrow {}^2D_{5/2}(m = \pm 5/2)$ are chosen and switched for a few times during the clock running. Fig. 2 shows the clock stability measurement during the 31-day-long clock comparison. The stability for a single clock is measured as $4.9(1)\times10^{-15}/\sqrt{\tau}$, and it reaches $6.3(^{+3.9}_{-1.4})\times10^{-18}$ at averaging time of 524000 s.

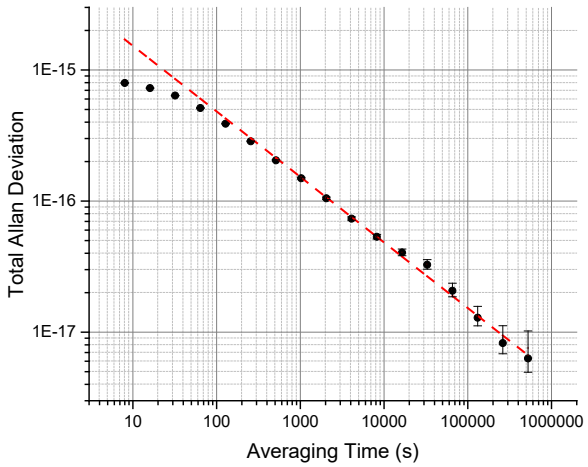

Fig 2. The total Allan deviation measured for a single clock (Feb. 25-Mar. 7, 2019). The measurement result is divided by $\sqrt{2}$ to represent the stability for a single clock. The red dash line shows the $1/\sqrt{\tau}$ fit of the data. The stability for a single clock is measured as $4.9(1)\times10^{-15}/\sqrt{\tau}$, and it reaches $6.3(^{+3.9}_{-1.4})\times10^{-18}$ at averaging time of 524000 s.

Fig. 3 shows the single clock total Allan deviation when the clock is locked to the $^2S_{1/2}(m=\pm1/2)\rightarrow{}^2D_{5/2}(m=\pm1/2)$ and $^2S_{1/2}(m=\pm1/2)\rightarrow{}^2D_{5/2}(m=\pm5/2)$ transition pairs during the last 10 days when the uptime is higher. As mentioned above, when locked to these transition pairs, it is more immune to the quadrupole shift variation. It is also proved in the experiment that the clock stability turns out to be better when locked to these transition pairs: the stability for a single clock is measured as $3.4(1)\times10^{-15}/\sqrt{\tau}$ during the last 10 days of clock comparison, reaching $7.9(^{+6.0}_{-1.8})\times10^{-18}$ at averaging time of 262000 s. Experiment also shows that the total Allan deviation is close to the theoretical predicted quantum projection noise limit, which is $2.2\times10^{-15}/\sqrt{\tau}$.

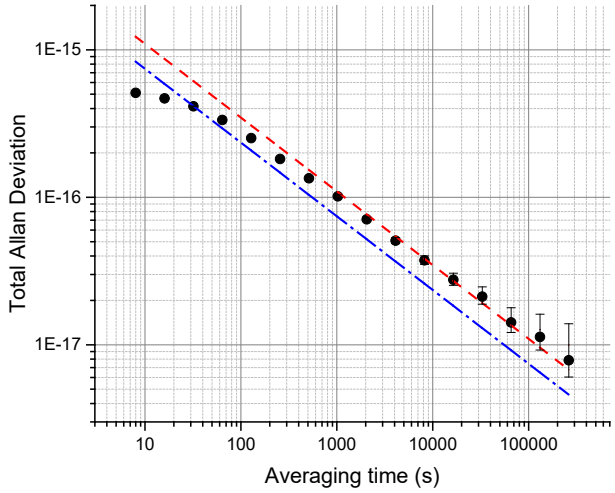

Fig. 3. The total Allan deviation measured for the two Ca^+ optical clocks when locked to the $^2S_{1/2}(m=\pm1/2)\rightarrow{}^2D_{5/2}(m=\pm1/2)$ and $^2S_{1/2}(m=\pm1/2)\rightarrow{}^2D_{5/2}(m=\pm5/2)$ transition pairs. The measurement result is divided by $\sqrt{2}$ to represent the stability for a single clock. The red dash line shows the $1/\sqrt{\tau}$ fit of the data. The stability for a single clock is measured as $3.4(1)\times10^{-15}/\sqrt{\tau}$, and it reaches $7.9(^{+6.0}_{-1.8})\times10^{-18}$ at averaging time of 262000 s. The blue dash line represents the theoretical predicted quantum projection noise limit of $2.2\times10^{-15}/\sqrt{\tau}$, calculated under the condition of 80-ms-long Ramsey method detection and 20% of dead time during each experiment cycle.

Discussion

In summary, in this paper, we reported on two Ca^+ optical frequency clocks with stabilities in the order of 10^{-18}. These clocks achieved stable, reliable, and long-term operation; moreover, in an operation period of around 10 days, their operation rate reached more than 90%. This high reliability was realized by enhancing the integration between the optical clock components and improving its

control software and hardware. In addition to meeting the requirement of a precision of 10^{-18} for optical clock frequency comparison, the high operating rate of these clocks could make them suitable for high-precision optical/hydrogen maser frequency comparisons, which, in turn, meets the prerequisites of optical clocks for International Atomic Time implementation. Grebing et al. reported that based on the high statistical resolution of the optical clock and using a high-bandwidth system, the frequency of a hydrogen maser could be quickly corrected [11]; in particular, in that work, the authors used a discontinuously operating optical clock to control the hydrogen maser, thus improving the performance of the time scale. Using this abovementioned method combined with the quasi-continuous data obtained in the current study, an extrapolation algorithm could be used to improve the performance of the hydrogen maser when the optical clock is interrupted, which could significantly improve the accuracy or stability. However, to realize a time scale based on an optical clock, the optical clock must not be interrupted for several hours, because, otherwise, this will cause a frequency jump in the hydrogen maser. One solution to address this problem is to use two or more optical clocks simultaneously as references.

As for the stability of the clocks, it is now limited by the clock laser stability of $\sim 8\times10^{-16}$. The clock laser stability is limited by the thermal noise limit of the 10-cm-long reference cavity. Reference cavities with lower thermal noise limit are now under development, made from 30-cm-long ULE spacers and Fused silica mirrors. The new reference cavities have thermal noise limit as low as $\sim 1\times10^{-16}$. By taking advantage of the clock lasers with stability of 1×10^{-16}, the clock stability is expected to be 2~3 times better. For even better stability, other techniques will be introduced, one of which is taking multiple ions as a reference instead of one. This will be challenging since making the systematic shifts for each ion identical in the ion trap is difficult, especially for the micromotion effect and the quadruple shift.

The experimental results reported in this paper indicated that the Ca^+ optical clock has a stability in the order of 10^{-18} on a time scale of hundreds of thousands of seconds, alluding that it is possible to achieve high-precision measurements on a long-time scale using the Ca^+ optical clock. Compared with other types of optical clocks with higher precision, Ca^+ optical clocks are characterized by a simple structure, low cost, easy integration, and suitability for miniaturization, making them useful for integrated and commercial applications. In addition, the method described in this paper is employed to measure a reliable optical local oscillator through a femtosecond optical comb and realize an optical clock time scale. Thus, this work demonstrates that it is possible to replace a microwave clock time scale with an optical clock time scale for higher accuracy and stability in the future.

Methods

Improvement made for better clock stability

New trap design and hardware setup for the clock In contrast to the ring-shaped Paul trap employed in Clocks 1 and 2, we used a microchip-level linear trap in Clock 3; we adopted the design used in Al^+ optical clocks [1,24], with only minor modifications. In particular, the linear trap is built of a 0.3-mm-thick piece of diamond, which is cut using a laser and then gold-plated to be used as an ion-trap electrode. The distances between the trapped ion and radio frequency electrodes are ~0.25 mm. The use of laser cutting to fabricate the trap electrode ensures fabrication precision,

allowing for a more symmetrical ion trap structure and more ideal trapping potential. Our experiment results indicate that this structure significantly reduced the heating rate of the ion trap. As an electrical insulator with extremely high thermal conductivity, diamond is an ideal material for an ion trap substrate; its high thermal conductivity ensures thermal uniformity in the ion trap and helps to further reduce the temperature uncertainty of the trap. As previously specified, the uncertainties of current Ca^+ optical clocks are dominated by the temperature evaluation uncertainty, the new ion trap design is expected to reduce the overall uncertainty of the optical clock. The main body of the vacuum system is composed of an octagon chamber with a diameter of < 100 mm. In addition, one CF35 window is included on the top for image collection and vertical laser probing, six CF16 windows are included on the sides for laser cooling/probing in the corresponding directions, and two CF16 feedthroughs are used for applying voltages on the trapping rf and compensation electrodes. Compared with Clock 2, the vacuum system in Clock 3 is smaller. Furthermore, as Clock 3 has more windows than Clock 2, three-dimensional (3D) measurements of micromotion or secular motion amplitudes can be easily realized by probing the motional sidebands, which could effectively increase the motional systematic shift evaluation precision. Similar to Clock 2, in Clock 3, a double-layer magnetic shielding system was adopted to significantly weaken the impact of environmental magnetic field fluctuations on the detection of the clock transition spectrum. In both clocks, within the magnetic shield, three pairs of coils are installed through which electric current is applied to set the amplitude and direction of the magnetic field for the experiment. In Clock 3, laser ablation technique is adopted for generating ions directly, whereas, in Clock 2, a heated atom furnace and photo-ionization are used to generate atoms; it is noteworthy that the laser ablation technique can generate ions within a few seconds without the need for photo-ionization lasers.

Improvements made for the cooling laser systems For Ca^+ clock, the cooling laser at 397 nm and the repumping laser at 866 nm are used for laser cooling. The transfer cavity technique was used for the laser frequency stabilization before. The cooling and repumping lasers are frequency stabilized to the clock laser using the transfer cavity. The advantage of this technique is the long-term stability is as good as the clock laser, however, the disadvantage is the technique wouldn't narrow the laser linewidth, and most of the time the linewidth at 0.1 s is measured as > 10 MHz, which makes the laser cooling efficiency lower. Now for both clocks, the ultra low thermal expansion (ULE) cavities are used for the laser frequency stabilization. The ULE cavities are made with finesse of ~ 100, linewidth and day drift of < 100 kHz are measured by beating the two individual lasers. Besides, Field Programmable Gate Array controlled Direct Digital Synthesis (DDS)s are introduced for tuning the rf applied to the acousto-optic modulators (AOM)s, which are used for tuning the laser frequencies. The DDSs' frequency and amplitude can be changed during the clock running, which is helpful for the optimization of the Doppler cooling. 0.5 ms of the near detuned, unsaturated Doppler cooling stage is introduced right after a 1.2 ms far detuned precool stage. Finally, by measuring the secular sideband amplitude, the ion's Temperature after Doppler cooling is evaluated as 1.0(5) mK, close to the Doppler cooling limit of ~0.5 mK.

Heating rate measurements We also performed 3D sideband cooling, leading to drastic reduction in the ion's secular motion amplitude [24] for Clock 3 in 3D; the average number of phonons in every direction owing to this reduction is less than 0.1. Sideband cooling also helps precisely measuring of the heating rate of the ion trap: The ions are first cooled down close to motion ground

state; then, all lasers are turned off for a period of time, such that the ions will be heated only by the effect of stray electric fields. We can then detect the ion temperature via spectroscopic measurements. By measuring the relationship between the ion temperature after heating and the time period that the laser was off, the heating rate of the ion trap could be determined via linear fitting. The results for heating rates of ion traps in Clock 3 in 3D directions indicate that the heating rates in all directions are less than 5 quanta/s. This would benefit the evaluation accuracy for the thermal motion shifts, especially when longer probe time is needed for pursuiting better stability, whereas the laser cooling process has to be paused for avoiding the light shifts. In our case, with heating rate at a few quanta/s level and a probe time of ~ 100 ms, the thermal motion shift uncertainty due to the heating rate is as low as 10^{-19} level.

State preparation Back in 2015, state preparation is not applied during the clock running. Thus, when probing each one of the clock Zeeman transitions, it has 50% of probability when ion is at the correct ground state. In 2018, state preparation technique using 397 nm $\sigma^{\pm}$ circular polarized laser beams are introduced [25]. However, the state preparation with 397 nm $\sigma^{\pm}$ lasers requires stronger magnetic field, while stronger magnetic field would require higher current, and it turns out the current source becomes noisier when the output current goes higher. Thus in this work, the clock laser is used instead for state preparation, a magnetic field of ~ 0.2 μT is applied to split the Zeeman components, this method not only is insensitive to the laser polarization variation or magnetic field variation, but also would not require a specific purity laser polarization. As a result, it is found that state preparation with the clock laser is more effective than with 397 nm $\sigma^{\pm}$ lasers. The state preparation process with the clock laser goes as follows: firstly, the $^2S_{1/2}(m = \pm 1/2) \rightarrow {}^2D_{5/2}(m = \pm 1/2)$ transition is stimulated by a 0.7-ms-long clock laser pulse for clearing out the $^2S_{1/2}(m = \pm 1/2)$ state population, afterwards a 0.5-ms-long 854 nm quenching laser pulse is applied for resetting the ion back to the ground state. The above process is repeated for 5 times, afterwards, the probability of the ion stays at the correct state is > 95%.

Ramsey method introduced Compared to the Rabi method, the Ramsey method has its own advantages. With the same probe time used, narrower transition linewidth can be observed with the Ramsey method. For example, Fig. 4 shows both the Ramsey and the Rabi spectroscopy observed with a probe time of 80 ms. The Ramsey spectroscopy has a linewidth of ~6.4 Hz instead of ~10 Hz with Rabi spectroscopy. For improved clock stability, the Ramsey method is adopted for running the clocks, it is proved that this method would improve the clock stability by a factor of ~1.4 [26,27].

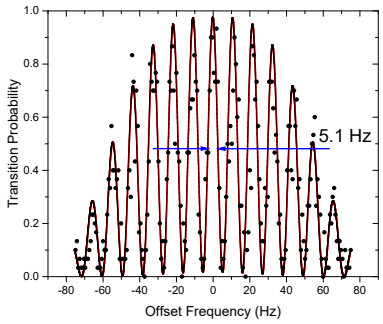

Ramsey

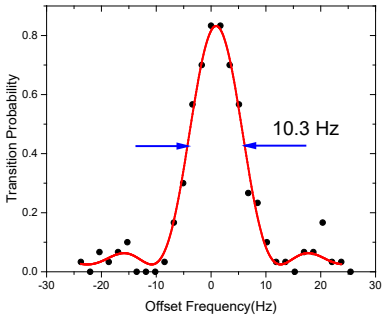

Rabi

Fig 4. Ramsey and the Rabi spectroscopy observed with a probe time of 80 ms. The observed transition linewidth is measured narrower with the Ramsey method, ~5.1 Hz compared to 10.3 Hz.

Improvement to the clock servo In order to reduce the influence of the nonlinear drift of the clock laser on the detection of clock transitions, the frequency drift was pre-compensated for in the locking experiment, i.e., the trend of the frequency drift was estimated via polynomial fitting and then compensated for using an AOM driven by a frequency synthesizer. The corresponding fitting parameters are used to analyze the variation trend in the frequency difference between the optical clock and laser; these parameters are updated once daily. The residual drift after compensation is less than 1 mHz/s. Considering this, the algorithm for the locking servo system used in the optical clock was improved; in addition, a high-order feedback compensation loop was added, which effectively suppressed the uncertainty introduced by the servo system. Consequently, the resulting frequency shift caused by the servo system was less than 2×10^{-18}. In the meantime, the new clock servo will change the frequency synthesizer output frequency or power much faster, making it possible for shorten the time interval between probing different clock transitions components with different m_J sub levels. The previous servo would keep probing a single component for as many as 30 times before switching to another component. While now the servo only probing a single component for as many as 30 times before switching to another, lowering the systematic uncertainty due to the residual Zeeman shift and the residual quadrupole shifts to the 10^{-19} level [20], which is a 2 orders of magnitude improvement [18].

Magnetic field optimization In our case for the $^{40}Ca^{+}$, the linear Zeeman shifts to the clock transition would be as strong as a few 10^{-11}/μT. While the linear Zeeman shift can be canceled out by probing symmetric Zeeman transition pairs, the magnetic field fluctuation would broaden the observed clock transition, keeping the clock stability from being any better. Two layers of magnetic shields are introduced to attenuates the magnetic field fluctuation, yet it turns out to be still not as good as expected. The magnetic field fluctuation in the vertical direction is much stronger than that in the horizontal directions, thus the magnetic field direction is set to be horizontal by adjusting the current on 3 pairs of magnetic field compensation coils. The overall magnetic field amplitude fluctuation is measured to be much smaller since when the magnetic field is set at the horizontal direction, the overall magnetic field amplitude is less sensitive to the vertical environmental magnetic field fluctuations.

References

[1] S. M. Brewer, J-S. Chen, A. M. Hankin, E. R. Clements, C. W. Chou, D. J. Wineland, D. B. Hume, D. R. Leibrandt, Phys. Rev. Lett. 123, 033201 (2019).

[2] T. L. Nicholson, S. L. Campbell, R. B. Hutson, G. E. Marti, B. J. Bloom, R. L. McNally, W. Zhang, M. D. Barrett, M. S. Safronova, G. F. Strouse, W. L. Tew, J. Ye, Nat. Commun. 6, 6869 (2015).

[3] Ichiro Ushijima, Masao Takamoto, Manoj Das, Takuya Ohkubo, Hidetoshi Katori, Nat. Photonics 9, 185 (2015).

[4] N. Huntemann, C. Sanner, B. Lipphardt, Chr. Tamm, E. Peik, Phys. Rev. Lett. 116, 063001 (2016).

[5] W. F. McGrew, X. Zhang, R. J. Fasano, S. A. Schäffer, K. Beloy, D. Nicolodi, R. C. Brown, N. Hinkley, G. Milani, M. Schioppo, T. H. Yoon, A. D. Ludlow, Nature 564, 87 (2018).

[6] Thomas P Heavner, Elizabeth A Donley, Filippo Levi, Giovanni Costanzo, Thomas E Parker, Jon H Shirley, Neil Ashby, Stephan Barlow, S R Jefferts, Metrologia 51, 174 (2014).

[7] R. Li, K. Gibble, K. Szymaniec, Metrologia 48, 283 (2011).

[8] S. Weyers, V. Gerginov, N. Nemitz, R. Li, K. Gibble, Metrologia 49, 82 (2012).

[9] Fritz Riehle, Patrick Gill, Felicitas Arias, Lennart Robertsson, Metrologia 55, 188 (2018).

[10] H. Hachisu, T. Ido, J. Appl. Phys. 54, 112401 (2015).

[11] Christian Grebing, Ali Al-Masoudi, Sören Dörscher, Sebastian Häfner, Vladislav Gerginov, Stefan Weyers, Burghard Lipphardt, Fritz Riehle, Uwe Sterr, Christian Lisdat, Optica 3, 563 (2015).

[12] Hidekazu Hachisu, Gérard Petit, Fumimaru Nakagawa, Yuko Hanado, Tetsuya Ido, Opt. Express 25, 8511 (2017).

[13] Charles F. A. Baynham, Rachel M. Godun, Jonathan M. Jones, Steven A. King, Peter B. R. Nisbet-Jones, Fred Baynes, Antoine Rolland, Patrick E. G. Baird, Kai Bongs, Patrick Gill et al, J. Mod. Opt. 65, 585 (2017).

[14] Jérôme Lodewyck, Sławomir Bilicki, Eva Bookjans, Jean-Luc Robyr, Chunyan Shi, Grégoire Vallet, Rodolphe Le Targat, Daniele Nicolodi, Yann Le Coq, Jocelyne Guéna, Michel Abgrall, Peter Rosenbusch, Sébastien Bize, Metrologia 53, 1123 (2016).

[15] Takumi Kobayashi, Daisuke Akamatsu, Kazumoto Hosaka, Yusuke Hisai, Masato Wada, Hajime Inaba, Tomonari Suzuyama, Feng-Lei Hong, Masami Yasuda, Metrologia 57, 065021 (2020).

[16] E. Oelker, R. B. Hutson, C. J. Kennedy, L. Sonderhouse, T. Bothwell, A. Goban, D. Kedar, C. Sanner, J. M. Robinson, G. E. Marti et al, Nat. Photonics, 13, 714 (2019).

[17] Christian Sanner, Nils Huntemann, Richard Lange, Christian Tamm, Ekkehard Peik, Marianna S. Safronova, Sergey G. Porsev, Nature 567, 204 (2019).

[18] Y. Huang, H. Guan, P. Liu, W. Bian, L. Ma, K. Liang, T. Li, K. Gao, Phys. Rev. Lett. 116, 013001 (2016).

[19] Yao Huang, Hua Guan, Mengyan Zeng, Liyan Tang, Kelin Gao, Phys. Rev. A 99, 011401 (R) (2019).

[20] Yao Huang, Huaqing Zhang, Baolin Zhang, Yanmei Hao, Hua Guan, Mengyan Zeng, Qunfeng Chen, Yige Lin, Yuzhuo Wang, Shiying Cao, Kun Liang, Fang Fang, Zhanjun Fang, Tianchu Li, Kelin Gao, Physical Review A 102, 050802(R) (2020).

[21] D. J. Berkeland, J. D. Miller, J. C. Bergquist, W. M. Itano, D. J. Wineland, J. Appl. Phys. 83, 5025 (1998).

[22] P. Dubé, A. A. Madej, J. E. Bernard, L. Marmet, J.-S. Boulanger, S. Cundy, Phys. Rev. Lett. 95, 033001 (2005).

[23] H. S. Margolis, G. P. Barwood, G. Huang, H. A. Klein, S. N. Lea, K. Szymaniec, P. Gill, Science 306, 1355 (2004).

[24] J.-S. Chen, S. M. Brewer, C. W. Chou, D. J. Wineland, D. R. Leibrandt, and D. B. Hume Phys. Rev. Lett. 118, 053002 (2017).

[25] Meng-Yan Zeng, Yao Huang, Hu Shao, Miao Wang, Hua-Qing Zhang, Bao-Lin Zhang, Hua

Guan, Ke-Lin Gao, Chinese Physics Letters 35, 074202 (2018).

[26] Baolin Zhang, Yao Huang, Yanmei Hao, Huaqing Zhang, Mengyan Zeng, Hua Guan, Kelin Gao, J. Appl. Phys. 128, 143105 (2020).

[27] P. Dubé, A. A. Madej, A. Shiner, B. Jian, Phys. Rev. A 92, 042119 (2015).

Acknowledgments

We thank J. Ye, Z. Fang, Y. Lin for help and fruitful discussion. This work is supported by the National Key R&D Program of China (Grant Nos. 2017YFA0304401, 2017YFA0304404, 2018YFA0307500, 2017YFF0212003), the Natural Science Foundation of China (Grant Nos. 11774388, 11634013), the Strategic Priority Research Program of the Chinese Academy of Sciences (Grant No. XDB21030100), CAS Youth Innovation Promotion Association (Grant Nos. 2018364, Y201963), and the K. C. Wong Education Foundation.

All authors edited and commented on the manuscript. Y. H., B. Z., M. Z., H. Z., Y. H., Z. C., and M.W. designed and performed the experiment, including analyzing the experimental data. B. Z. wrote the program for the experiment. Y. H., H. G., and K. G. supervised the work. Y. Huang wrote the manuscript.

Competing Interests

The authors declare that they have no competing financial interests. Readers are welcome to comment on the online version of the paper.

Correspondence

Correspondence and requests for materials should be addressed to K. G. (email: klgao@wipm.ac.cn) or H. G. (guanhua@wipm.ac.cn)

Figures

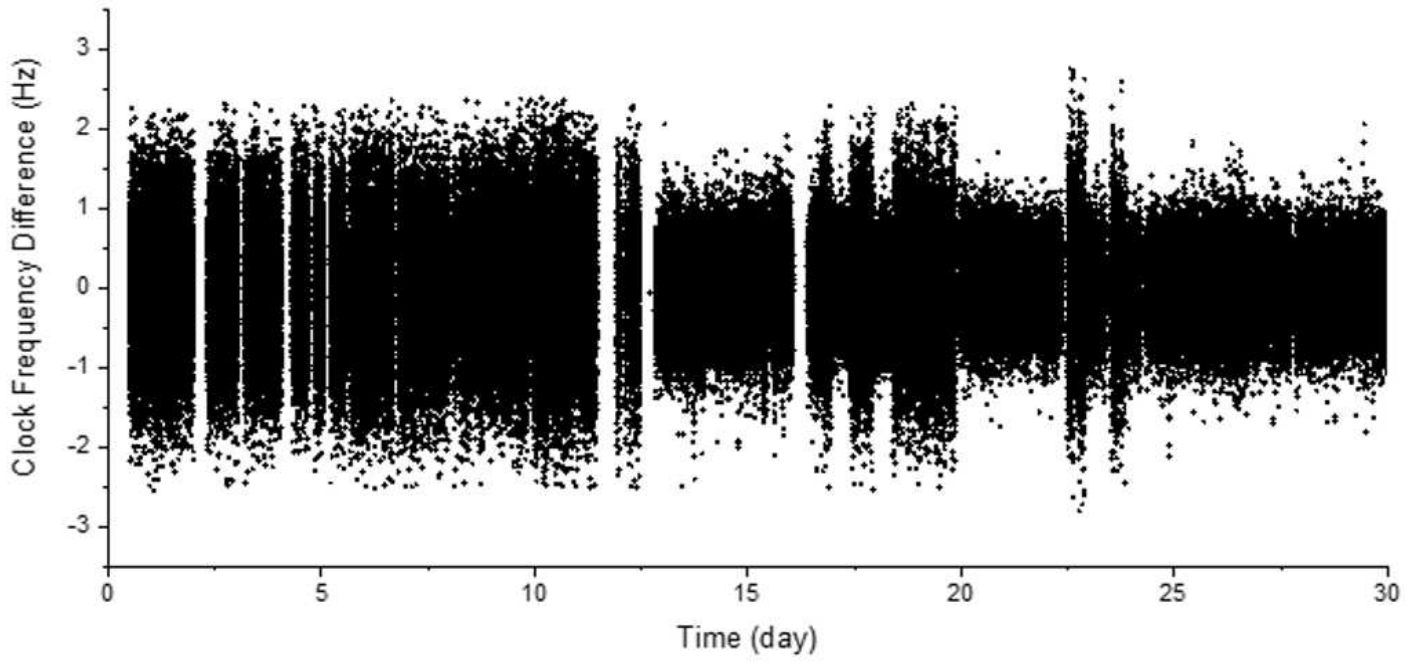

Figure 1

the frequency difference measured of the two clocks. Each data point shows the frequency difference average in an 8-s-long experiment. During the 31-day-long clock comparison, transition pairs 2S1/2(m=±1/2)↔2D5/2(m=±1/2) and 2S1/2(m=±1/2)↔2D5/2(m=±3/2), or 2S1/2(m=±1/2)↔2D5/2(m=±1/2) and 2S1/2(m=±1/2)↔2D5/2(m=±5/2 are chosen and switched for a few times during the clock running. The overall uptime percentage is ~73%, during the last 5 days, the uptime is >90%.

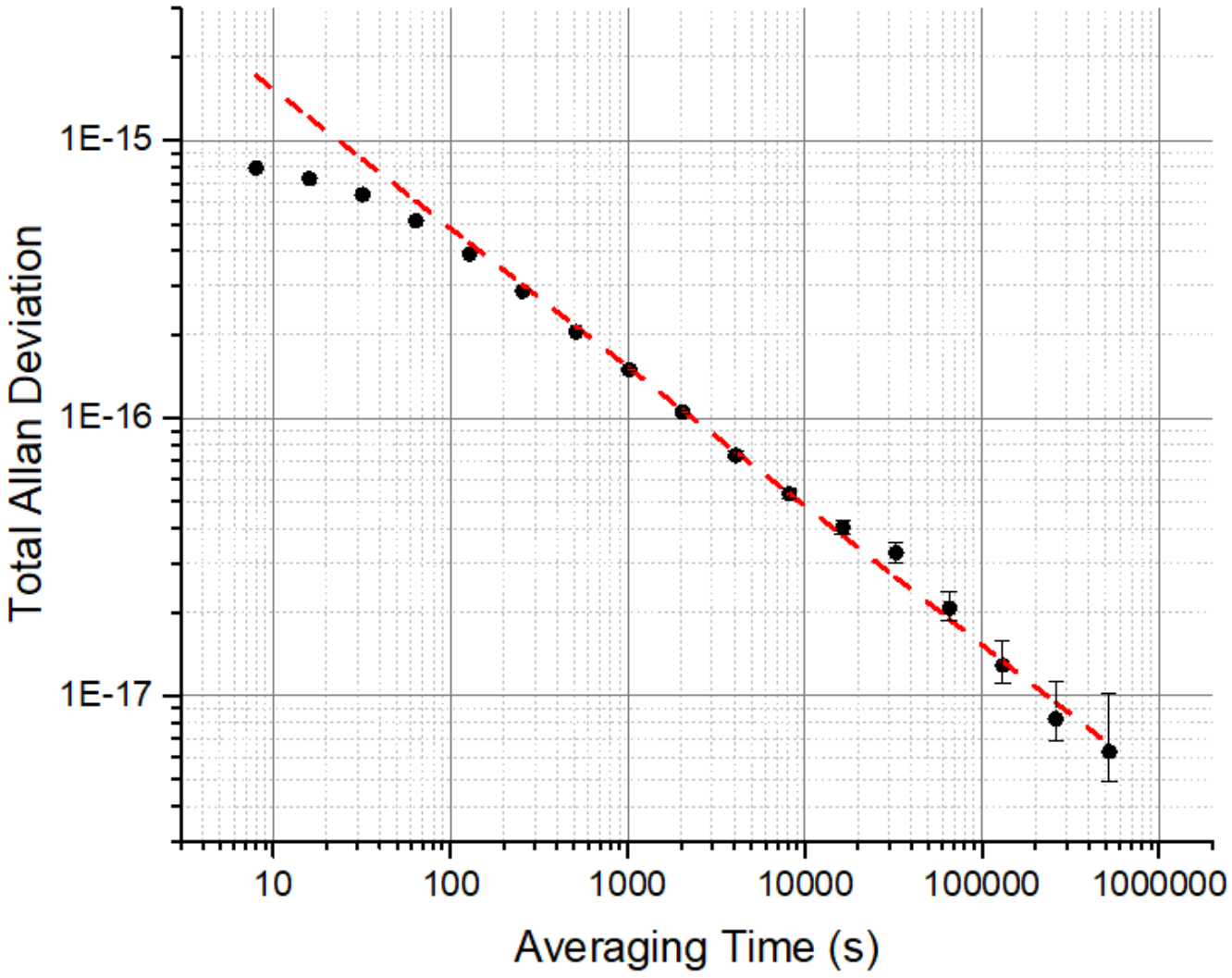

Figure 2

The total Allan deviation measured for a single clock (Feb. 25-Mar. 7, 2019). The measurement result is divided by √2 to represent the stability for a single clock. The red dash line shows the 1/√τ fit of the data. The stability for a single clock is measured as 4.9(1)×10-15/√τ, and it reaches 6.3((+3.9@-1.4))×10-18 at averaging time of 524000 s.

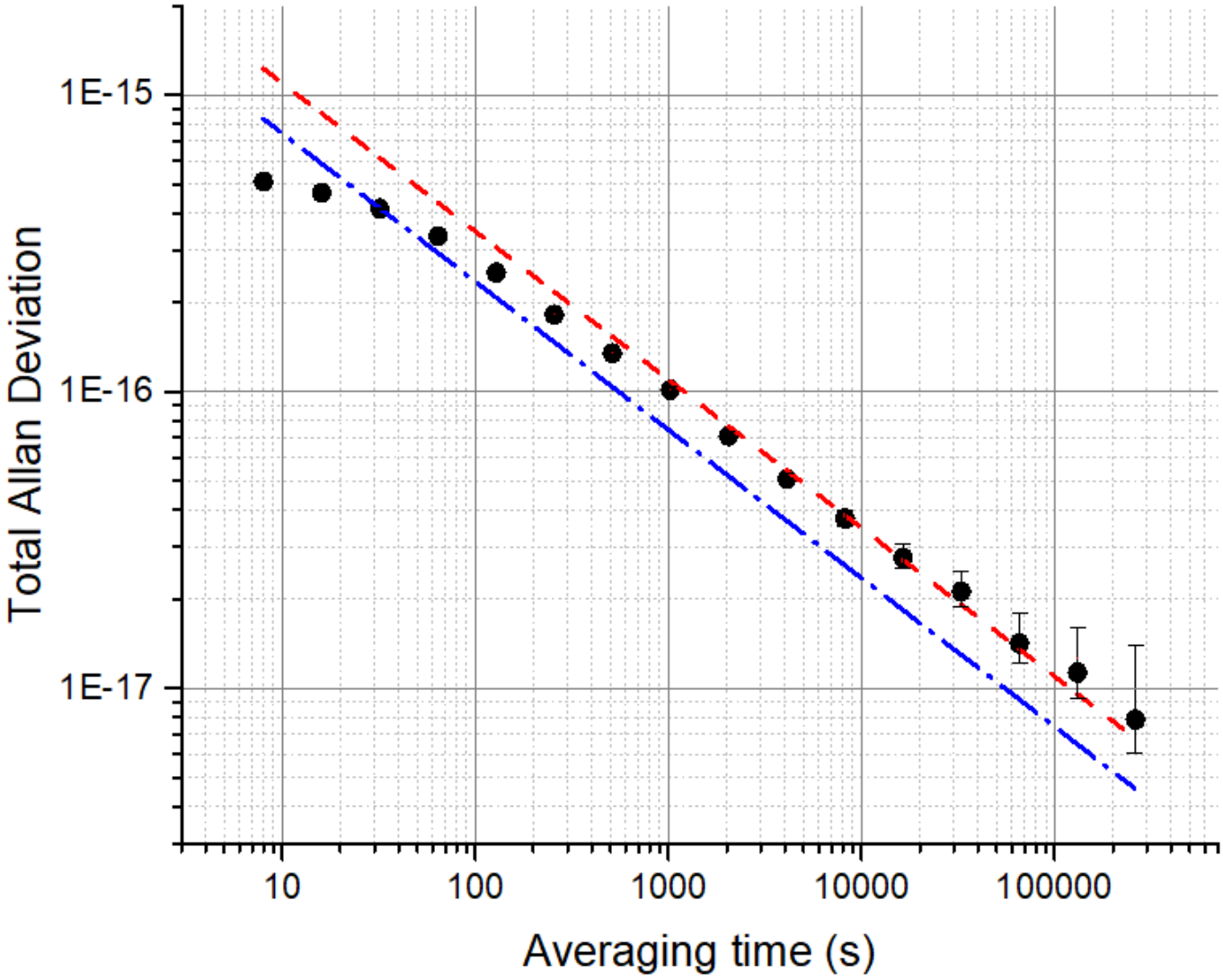

Figure 3

The total Allan deviation measured for the two Ca+ optical clocks when locked to the 2S1/2(m=±1/2)⟷2D5/2(m=±1/2) and 2S1/2(m=±1/2)⟷2D5/2(m=±5/2) transition pairs. The measurement result is divided by √2 to represent the stability for a single clock. The red dash line shows the 1/√τ fit of the data. The stability for a single clock is measured as 3.4(1)×10-15/√τ, and it reaches 7.9((+6.0@-1.8))×10-18 at averaging time of 262000 s. The blue dash line represents the theoretical predicted quantum projection noise limit of 2.2×10-15/√τ, calculated under the condition of 80-ms-long Ramsey method detection and 20% of dead time during each experiment cycle.

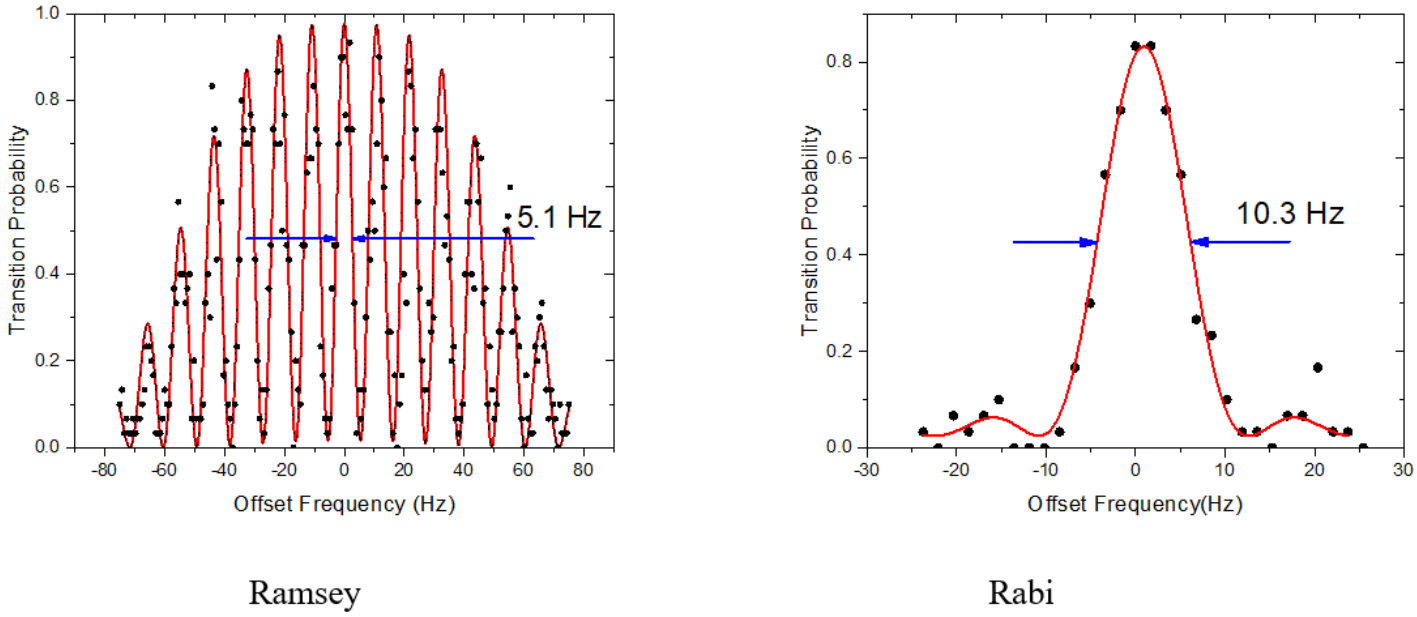

Figure 4

Ramsey and the Rabi spectroscopy observed with a probe time of 80 ms. The observed transition linewidth is measured narrower with the Ramsey method, ~5.1 Hz compared to 10.3 Hz.